Electronic Supplementary Material (ESI) for Physical Chemistry Chemical Physics.
This journal is © the Owner Societies 2017

SUPPORTING INFORMATION

Room-temperature in-cell EPR spectroscopy: Alpha-Synuclein disease variants remain intrinsically disordered in the cell

Julia Cattani,[†] Vinod Subramaniam,[†,‡] and Malte Drescher*,[†]

[†] *Department of Chemistry and Konstanz Research School Chemical Biology, University of Konstanz, 78457 Konstanz, Germany*

[‡] *Vrije Universiteit Amsterdam, De Boelelaan 1105, 1081 HV Amsterdam, The Netherlands*

E-mail: malte.drescher@uni-konstanz.de

CONTENTS

A. METHODS AND MATERIALS 4
1. Protein expression and Site Directed Spin Labeling 4
2. Preparation of protein fibrils 5
3. Atomic Force Microscopy 5
4. Preparation of vesicles 5
5. Sample Preparation for EPR measurement with LUVs 5
6. Dynamic Light Scattering 5
7. Circular Dichroism 6
8. Preparation for in-cell EPR 6
9. Cw-EPR measurements 6
10. Double electron-electron resonance (DEER) measurements 7
B. DATA ANALYSIS AND EXPERIMENTAL RESULTS 8
1. Spectral Fitting of reference spectra 8
2. aS conformations under controlled conditions: control experiments 11
3. Data analysis of cw-EPR spectra 14
4. Intracellular spatial distribution of aS 18
5. Stability and line shape of the in cell nitroxide signal 19
6. 4-Oxo-Tempo as viscosity control inside the cell 20
7. Comparison of in-cell EPR spectra and spectra in aqueous solution 22
8. Comparison of in-cell wilde-type aS with A30P and A53T 25
9. Quantitative spectral analysis of the intracellular experiments 26
C. REFERENCES 28

LIST OF FIGURES

Figure S1. Amino acid sequence of A) aS, B) A30P and C) A53T 4
Figure S2. CD spectra of wt-aS, A30P and A53T as well as mutants singly labeled at residue 9, 27, 56, 90 in buffer. 11
Figure S3. DLS data of POPG LUVs after extrusion and with bound wt-aS. 12
Figure S4. CD spectra of wt-aS, A30P and A53T as well as mutants singly labeled at residue 9, 27, 56, 90 bound to LUVs.CD spectra of aS fibrils in buffer. 12
Figure S5. AFM images of aS fibrils (wtaS:aS9 = 20:1) 13
Figure S6 AFM images of aS fibrils (wtaS:aS69 = 20:1) 13
Figure S7. CD spectra of aS fibrils in buffer. 13
Figure S8. Signal-to-Noise-Ratio (SNR) of the accumulated cw-EPR spectral slices. 14
Figure S9. Cw-EPR spectrum of oocyte background before and after smoothing. 14
Figure S10. Accumulated cw-EPR spectra of aS mutants injected into oocytes of *Xenopus laevis*, smoothed oocytes background and background-corrected spectra. 15
Figure S11. Accumulated cw-EPR spectra of A30P mutants injected into oocytes of *Xenopus laevis*, smoothed oocytes background and background-corrected spectra. 16

Figure S12. Accumulated cw-EPR spectra of A53T mutants injected into oocytes of *Xenopus laevis* (black), smoothed oocytes background (blue) and background-corrected spectra (red).. 17
Figure S13. Four pulse DEER-traces of A30P-41 in oocytes and Proxyl in Tris-HCl. 18
Figure S14. Signal decay over time of A30P-41 injected into oocytes. 19
Figure S15. Cw-EPR specra of A53T-56 injected into oocytes at different time points. 19
Figure S16. Cw-EPR spectrum of 4-Oxo-Tempo (Tempone) in buffer and injected into oocytes.... 20
Figure S17. Cw-EPR spectrum of 4-Oxo-Tempo in buffer, corresponding simulation and simulation with increased rotational correlation time τ. 20
Figure S18. Cw-EPR spectra of aS (labeled at varios positions) in buffer and injected into oocytes. 22
Figure S19. Cw-EPR spectra of A30P (labeled at varios positions) in buffer and injected into oocytes. 23
Figure S20. Cw-EPR spectra of A53T (labeled at varios positions) in buffer and injected into oocytes. 24
Figure S21. Cw-EPR spectra of wt-aS, A30P and A53T (labeled at varios positions) injected into oocytes. 25
Figure S22. Spectral Simulation of aS9 with different alpha-helical content compared to intracellular aS9. 26
Figure S23. Spectral Simulation of aS69 with different fibril content compared to intracellular aS69. 27

SUPPLEMENTARY TABLES OVERVIEW .....

Table S1. Simulation parameters of aS9 and aS69 in Tris-HCl buffer. 8
Table S2. Simulation parameters of the fast component SA and slow component SB of aS9 on POPG LUVs..... 8
Table S3. Simulation parameters of the fast component SA and slow component SB of aS69 on POPG LUVs..... 9
Table S4. Simulation parameters of aS9 fibrils using a four component fit..... 9
Table S5. Simulation parameters of aS69 fibrils using a four component fit..... 10
Table S6. Simulation parameters of 4-Oxo-Tempo in buffer and simulation for viscosity change. 21

A. METHODS AND MATERIALS

1. Protein expression and Site Directed Spin Labeling

```
A   10        20        30        40        50
    MDVFMKGLSK AKEGVVAAAE KTKQGVAEAA GKTKEGVLYV GSKTKEGVVH
    60        70        80        90        100
    GVATVAEKTK EQVTNVGGAV VTGVTAVAQK TVEGAGSIAA ATGFVKKDQL
    110       120       130       140
    GKNEEGAPQE GILEDMPVDP DNEAYEMPSE EGYQDYEPEA

B   10        20        30        40        50
    MDVFMKGLSK AKEGVVAAAE KTKQGVAEAP GKTKEGVLYV GSKTKEGVVH
    60        70        80        90        100
    GVATVAEKTK EQVTNVGGAV VTGVTAVAQK TVEGAGSIAA ATGFVKKDQL
    110       120       130       140
    GKNEEGAPQE GILEDMPVDP DNEAYEMPSE EGYQDYEPEA

C   10        20        30        40        50
    MDVFMKGLSK AKEGVVAAAE KTKQGVAEAA GKTKEGVLYV GSKTKEGVVH
    60        70        80        90        100
    GVTTVAEKTK EQVTNVGGAV VTGVTAVAQK TVEGAGSIAA ATGFVKKDQL
    110       120       130       140
    GKNEEGAPQE GILEDMPVDP DNEAYEMPSE EGYQDYEPEA
```

Figure S1. Amino acid sequence of A) aS, B) A30P and C) A53T. The point mutations of A30P and A53T are marked in red, the positions for cysteine substitution and 3-maleimido-proxyl labeling are marked in green.

Alpha-Synuclein consists of 140 amino acids as depicted in Figure S1. Wild-type aS, A30P and A53T do not contain any cysteine residues. aS, A30P and A53T cysteine-mutations at sites 9, 18, 27, 35, 41, 56, 69, 90, 140 (shown in green in Figure S1), respectively, have been introduced using standard biochemical methods.[1] aS mutants were expressed in *Escherichia coli* strain BL21(DE3) using the pT7-7 expression plasmid (courtesy of the Landsbury Laboratory, Harvard Medical School, Cambridge, MA). The protein was purified using 1 mM DTT. Prior to labeling, the protein was reduced with a 6x molar excess of DTT over -SH groups for 30 minutes at room temperature. Afterwards, DTT was removed using Pierce Zeba 2 mL desalting columns and a 3x molar excess of 3-maleimido-PROXYL spin label (3-Maleimido-2,2,5,5-tetramethyl-1-pyrrolidinyloxy) (Sigma Aldrich Co. LLC) was immediately added and the protein solution was incubated for two hours in the dark at room temperature. Subsequently, free label was removed by using two additional desalting steps. To achieve final protein concentrations of about 1 mM Vivaspin 2 10000 MWCO filters were used.

The labeling efficiency was experimentally determined by measuring the spin label concentration via cw-EPR and measuring the protein concentration using a Nanodrop 1000 spectrophotometer (Thermo Scientific). The obtained labeling efficiency is in the range of 60-100 %. Samples were kept on ice during the washing process to minimize aggregation and stored at -80 °C afterwards.

2. Preparation of protein fibrils

Aggregation reactions were set up with 100 µM aS (diamagnetic ratio wt:aS9 = 20:1 and wt:aS69 = 20:1) in Tris-HCl (10mM, pH 7.4, 100 µM EDTA, 150 mM NaCl) with a volume of 100 µL. The solution was incubated at 37 °C shaking with 1000 rpm for two weeks.
After incubation, the solution was sonicated for 10 min using a bath sonicator (Elmasonic S10H, 220-240 V, 90 W, Elma, Singen).

3. Atomic Force Microscopy

AFM samples were prepared by adsorbing 20 µL of the sonicated fibril solution on a freshly cleaved mica plate (Muscovite mica, V-1 quality, EMS) for 4 min and washing five to six times with 100 µL Milli-Q water and drying under a gentle stream of nitrogen gas.
AFM images were recorded on a Multimode Microscope (Bruker Biospin, Karlsruhe) in soft tapping mode with an Otespa-R3 tip (Bruker). All images were acquired with a resolution of 1024 x 1024 pixels per image. Images were analyzed by Gwyddion 2.46 data analysis software.

4. Preparation of lipid vesicles

Anionic POPG [1-palmitoyl-2-oleoyl-sn-glycero-3-phospho-(1'-rac-glycerol)] was purchased in chloroform solution from Avanti Polar Lipids (Birmingham, AL). 500 µL lipid stock solution of POPG were put under a gentle stream of nitrogen to remove the chloroform. The resulting lipids films were placed under vacuum overnight and then rehydrated in a volume of 300 µM of Tris-HCl buffer (10 mM, pH 7.4) to a final concentration of around 40 mM lipid and incubated 30 min at room temperature.
LUVs were prepared by repetitive extrusion through one layer of 100 nm polycarbonate film in a handheld extruder (Avanti, Polar Lipids). The average diameter of LUVs was about 100 nm, as measured by dynamic light scattering (see below). The total phospholipid concentration was determined according to the protocol of Chen et al.[2]. Vesicles were used within 5 days of preparation but were found to be structurally stable for at least two weeks when stored at 4 °C.

5. Sample Preparation for EPR measurement with lipid vesicles

Spin-labeled aS solution in Tris-HCl buffer (10 mM, pH 7.4, protein concentration between 150-250 µM) was added to the liposome solution resulting in a protein:lipid-ratio of 1:250 and a final protein concentration of approximately 50 µM. The mixture was allowed to incubate for at least 30 minutes at 293 K before starting transferring it into a glass capillary (ringcaps, Hirschmann Laborgeräte) that was fused at one side by using a microliter syringe (Hamilton). Following this step, the capillary was placed in a 2 mm EPR guiding tube (Bruker Biospin) and inserted into the resonator of the spectrometer before starting the measurement.

6. Dynamic Light Scattering

Vesicle size and stability of LUVs in Tris-HCl buffer and upon interaction with aS were studied by Dynamic Light Scattering (DLS). The DLS studies were performed at
25 °C using a Malvern Zetasizer nano ZS spectrometer (Malvern Instruments Ltd), equipped with a 4 mW He-Ne laser (vertically polarized incident radiation of wavelength 633 nm). The
solution containing LUVs (2 µl) was dispensed in 1 ml Tris-HCl buffer (10 mM, pH 7.4) into a 1 cm polycarbonate cuvette.
For the measurement of the LUVs upon aS addition the samples used for the circular dichroism measurements were recollected. 2 µL of the recollected solution of dispensed in 1 mL Tris-HCl buffer (10 mM, pH 7.4) into a 1 cm polycarbonate cuvette.

7. Circular Dichroism

CD measurements (180 to 260 nm, 1 nm bandwidth, and continuous mode with a scanning rate of 50 nm/min) were recorded on a Jasco J815 spectropolarimeter (Jasco Analytical Instruments). Spectra were taken at 20 °C in 0.5 mm demountable cuvettes (Hellma, Forest Hills, NY).

Samples with a protein concentration of approximately 0.2 mg/ml protein in Tris-HCl buffer in the absence or presence of POPG LUVs (4.0 mg/ml lipid concentration) after 30 min incubation at room temperature, and of aS fibrils with an aS concentration of 30 µM in Tris-HCl (10 mM, pH 7.4, 100 µM EDTA, 150 mM NaCl) were measured.

Five scans per sample were averaged for pure protein and spectra with LUVs. For aS fibril spectra ten scans were averaged. Baseline correction, subtraction of the background spectrum and smoothing was applied to the raw data. Data of aS and its variants in buffer and with LUVs were normalized using Origin (OriginLab, Northampton, MA).

8. Preparation for in-cell EPR

The *Xenopus laevis* oocytes on stage V/VI (purchased from EcoCyte Bioscience, Caustrop-Rauxel) were kept in MBS (modified Barth's saline, 1x: 88 mM NaCl, 1 mM KCl, 1 mM $MgSO_4$, 5mM HEPES (2-[4-(2-hydroxyethyl)piperazin-1-yl]ethanesulfonic acid), 2.5 mM $NaHCO_3$, 0.7 mM $CaCl_2 \cdot H_2O$) at 18 °C.

Prior to the microinjection, about ten oocytes were prepared on a home-made poly-(tetrafluoroethylene) holder in MBS (1x) and visually controlled before usage. 50.6 nL of the 1mM protein solution in Tris-HCl buffer (10mM, pH 7.4) was microinjected into the oocytes using a Nanoject II automatic nanoliter injector with fitting micromanipulator MM33 (Drummond, Broomall, PA). Subsequently, the oocytes were washed carefully with MBS (1x). Five microinjected oocytes were then collected cautiously in a Q-band tube (quartz glass, 1 mm inner diameter, purchased from Bruker) via slightly negative pressure on one end of the tube. The oocytes were visually inspected before as well as after the EPR measurement using a Stemi 2000-C binocular microscope mounted with an AxiaCam ERc 5s camera (Zeiss, Oberkochen). After removing supernatant MBS, the sample tube was sealed with a capillary tube sealing compound (Cha seal, Kimble Chase Life Science and Research Products, LLC) at the top to guarantee a fixed sample position within the tube. The capillary was placed in a 2 mm EPR guiding tube (Bruker Biospin) and the EPR measurements were started immediately after preparation was finished (about 10 minutes after microinjection).

9. Cw-EPR measurements

All cw-EPR spectra were recorded in X-band (9.5 GHz microwave frequency) using an Elexsys E580 spectrometer equipped with a Super High-Q cavity probe head (both Bruker) at 293 K. The temperature was controlled using an ESR900 helium gas flow system (Oxford Instruments). We performed modulated field sweeps containing 2048 data points (sweep time 83.89 s) at a modulation frequency of 100 kHz. Modulation amplitude as well as time constant have been chosen such that the signal was not distorted. Typical values are 0.6 G and 40.96 ms, respectively. Spectrometer control was performed by the Bruker Xepr software.

Spectra in Tris-HCl buffer (10mM, pH 7.4) were recorded with 5-10 scans for each sample.

For the aS fibril measurements the spectra were recorded with a time delay of 100 ms between each scan. Each scan was saved individually, about 600 scans were recorded.

For the in-cell cw-EPR measurements the spectral scans were recorded with a time delay of 100 ms. After about 30-60 min the nitroxide signal had disappeared due to the cell environment and the measurement was stopped. After 3-6 h an additional measurement was started to determine the background signal of the oocytes (around 20 scans were accumulated).

10. Double electron-electron resonance (DEER) measurements

For double electron electron resonance (DEER) experiments[3] *Xenopus laevis* oocytes were prepared and injected as described in the section "**Preparation for in-cell EPR".** Upon microinjection, three oocytes were collected cautiously in a Q-band tube (quartz glass, 1 mm inner diameter, purchased from Bruker) via slightly negative pressure on one end of the tube. The oocytes were visually inspected directly afterwards using a Stemi 2000-C binocular microscope mounted with an AxiaCam ERc 5s camera (Zeiss, Oberkochen). After removing supernatant MBS and an incubation time of 15 min the sample tube was shock-frozen in liquid nitrogen, and stored at -80°C until further use.

The DEER measurement was performed in Q-band at 34 GHz using an Elexsys E580 spectrometer equipped with a EN 5107D2 Q-band EPR probe head (both Bruker Biospin) and a 10 W MW power solid state amplifier (HBH Microwave GmbH). The temperature was controlled with a CF935 helium gas flow system (Oxford Instruments). The four-pulse, dead-time free DEER sequence is given by: $\pi/2_{obs} - \tau_1 - \pi_{obs} - t - \pi_{pump} - (\tau_1+\tau_2-t) - \pi_{obs} - \tau_2 -$ echo. The echo amplitude is observed as a function of time *t* starting with *t* = 280 ns. The pump pulse (20 ns corresponding to a π-pulse) was set to the maximum of the nitroxide spectrum and the observer pulse was set 50 MHz higher; π/2 and π pulses at observer frequency were of around 40 ns and 20 ns length, respectively. The samples were measured at τ_2 = 2100 ns (A30P-41 in oocytes) and τ_2 = 3800 ns (Proxyl in Tris-HCl, 20 vol% Glycerol), τ_1 = 400 ns and a shot repetition time of 3.5 ms (A30P-41 in oocytes) and 5.5 ms (Proxyl in Tris-HCl, 20 vol% Glycerol. The accumulation time was typically 18 hours at 50 K.

B. DATA ANALYSIS AND EXPERIMENTAL RESULTS

1. Spectral Fitting of reference spectra

All fittings and spectral simulations were performed using Matlab R2016a (The MatWorks, Inc. Natrick, MA) and the toolbox EasySpin 5.0.20[3].

The spectra of aS9 and aS69 in Tris-HCl buffer (10mM, pH 7.4) were fitted using a one component fit with the EasySpin function *chili* using a linewidth of 0.13 mT and g-tensor [g_x g_y g_z] = [2.0105 2.0055 2.0029], other parameters are shown in Table S1.

Table S1. Simulation parameters of aS9 and aS69 in Tris-HCl buffer, simulation and experimental data are shown in Fig 1. All simulations were done with 0.13 mT linewidth.

	^{14}N Hyperfine coupling [MHz]		**Rotational correlation time [ns]**
	A_{xx}=A_{yy}	**A_{zz}**	**τ_r**
aS9	13	111	0.41
aS69	5	127	0.26

The spectrum of aS9 and aS69 bound on POPG LUVs was fitted (see Table S2 and S3) using a fit of two components with the EasySpin function *chili*. The spectrum can be described by a superposition S = (1-b) S_A + b S_B, where S_A is the fast component, S_B is the slow, bound component and b is the fraction of spectral component S_B.[4] The parameters of the fast component S_A were taken from the fit of the individual measurements of aS9 and S69 in buffer (see Table S1), respectively.

Table S2. Simulation parameters of the slow component S_B and the fast component S_A of aS9 on POPG LUVs, simulations and experimental data are shown in Fig 1. All simulations were done with 0.13 mT linewidth.

	^{14}N Hyperfine coupling [MHz]		**Rotational correlation time [ns]**	**Fraction**
	A_{xx}=A_{yy}	**A_{zz}**	**τ_r**	**b**
S_A	13	111	0.41	0.009
S_B	11	111	2.12	0.991

Table S3. Simulation parameters of the slow component S_B and the fast component S_A of aS69 on POPG LUVs, simulations and experimental data are shown in Fig 1. All simulations were done with 0.13 mT linewidth.

	^{14}N Hyperfine coupling [MHz]		Rotational correlation time [ns]	Fraction
	$A_{xx}=A_{yy}$	A_{zz}	τ_r	b
S_A	5	127	0.26	0.978
S_B	14	105	2.75	0.022

The spectra of aS9 fibrils and of as69 fibrils were simulated (see Table S4 and S5) using a four component fit (a fast (monomeric) component S_C and the slow oligomeric and fibril components S_D, S_E and S_G)[4] with the EasySpin function *chili*. This approach is not based on a physical model of the rotational behavior of the spin label in the fibril, which corresponds very likely to a more complicated motional model. The presented parameter set is very unlikely to fit a spectrum taken at high frequency if this will be done. However, for parameterizing the experimental data for later use in the spectral simulations shown in Fig. S21 and S22 (see part B, Chapter 9), the approach is well suited.

Table S4. Simulation parameters of aS9 fibrils using a four component fit, simulation and spectrum are shown in Fig 1. All simulations were done with 0.13 mT linewidth.

	^{14}N Hyperfine coupling [MHz]		Rotational correlation time [ns]	Fraction
	$A_{xx}=A_{yy}$	A_{zz}	τ_r	
S_C	30	88	0.30	0.183
S_D	17	100	1.19	0.034
S_E	16	96	1.53	0.268
S_G	10	85	6.08	0.515

Table S5. Simulation parameters of aS69 fibrils using a four component fit, simulation and spectrum are shown in Fig 1. All simulations were done with 0.13 mT linewidth.

	^{14}N Hyperfine coupling [MHz]		Rotational correlation time [ns]	Fraction
	$A_{xx}=A_{yy}$	A_{zz}	τ_r	
S_C	24	90	0.51	0.099
S_D	31	72	0.79	0.055
S_E	25	78	0.85	0.059
S_G	22	114	7.02	0.787

2. aS conformations under controlled conditions: control experiments

The EPR spectra of spin-labeled aS, shown in Figure 1 in the main script were obtained under controlled in vitro conditions.

In aqueous buffer

CD-spectra (Figure S2) of aS variants (wild-type and labeled) in buffer prove that labeling does not alter the conformational behavior because the spectral shape does not change upon labeling. Deviations in the spectral intensities reflect different concentrations. The spectral shape suggest an intrinsically disorder of aS in buffer. .

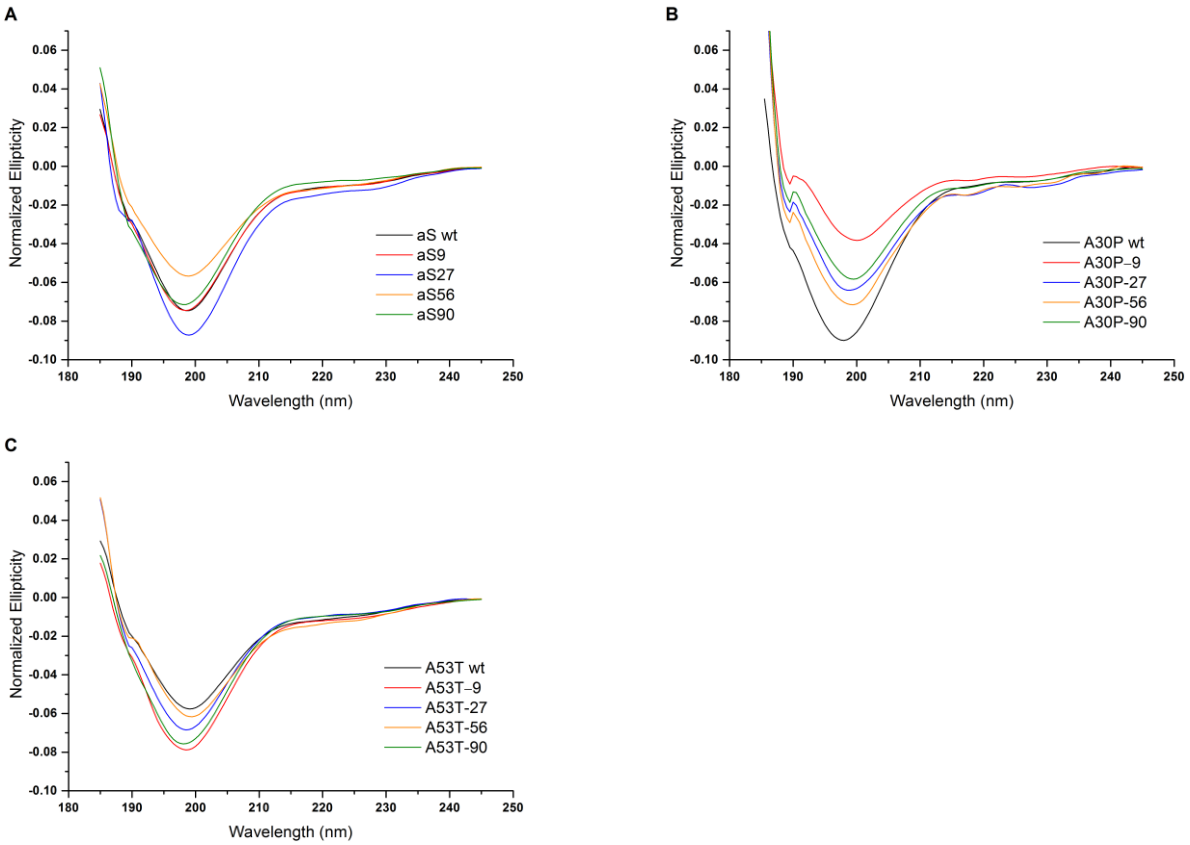

Figure S2. CD spectra of wt-aS (A), A30P (B) and A53T (C) as well as the corresponding molecules singly labeled at residue 9, 27, 56, 90 in Tris-HCl (10 mM, pH 7.4) buffer.

In the presence of negatively charged membranes

DLS data in Figure S3 (three independent measurements of the very same sample) of large unilamellar vesicles before (A) and after (B) addition of aS do not show significant changes. This proves that aS does not disrupt the large unilamellar vesicles under the applied conditions.[5] n
CD-spectra of aS in the presence of LUVs (Figure S4) prove that labeling does alter neither the membrane binding affinity nor the conformational behavior upon membrane binding because the spectral shape does not change upon labeling. The spectral shape suggests a mainly alpha-helical conformation.

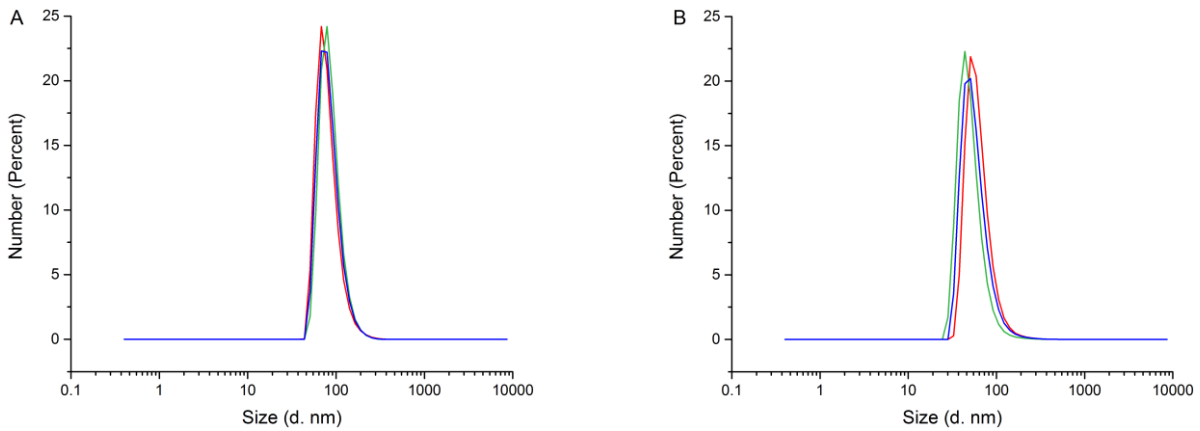

Figure S3. DLS data of POPG LUVs after extrusion (A) and upon addition of aS (B). Three independent measurements are shown (blue, green, red). The particle size distribution is depicted for logarithmically spaced size classes on the X-axis with relative percentage of particles in each size class on the Y-axis.

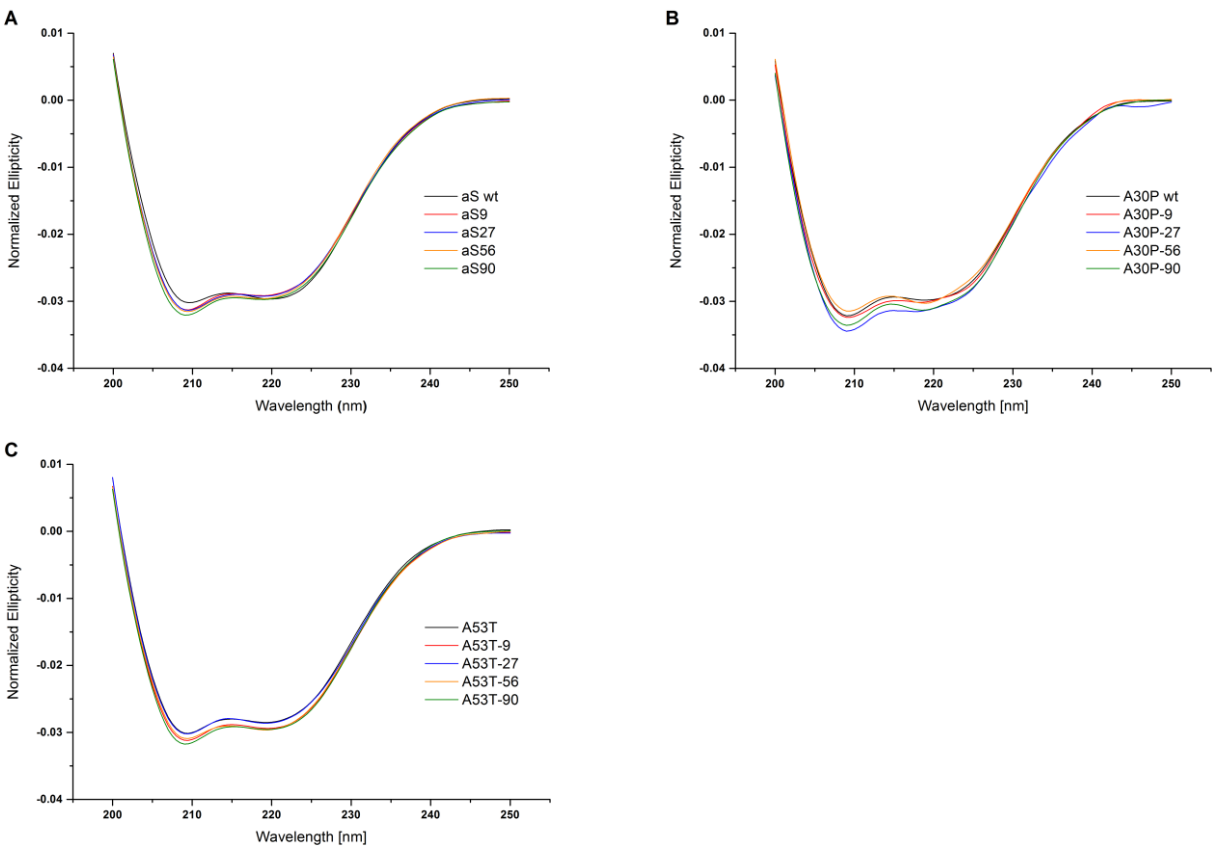

Figure S4. CD spectra of wt-aS (A), A30P (B) and A53T (C) as well as corresponding molecules singly labeled at residue 9, 27, 56, 90 after incubation with POPG LUVs. For concentration independent comparison of the spectral shape, normalized ellipticity values were used. The spectral shape does not differ significantly upon labeling.

<u>Upon fibrillization</u>

aS fibrils were grown and sonicated as described above. The grown fibrils were sonicated to obtain short oligomer fragments to prevent signal loss during the EPR measurement due to sedimentation. AFM images (Figure S5 and S6) show sonicated fibril fragments. Figure S7 shows CD spectra of sonicated aS fibrils. The CD data suggest beta-sheet structure of aS upon

fibrillization. Deviations in the spectral intensities derive from fluctuations in the concentrations and the demountable cuvettes used for the measurements.

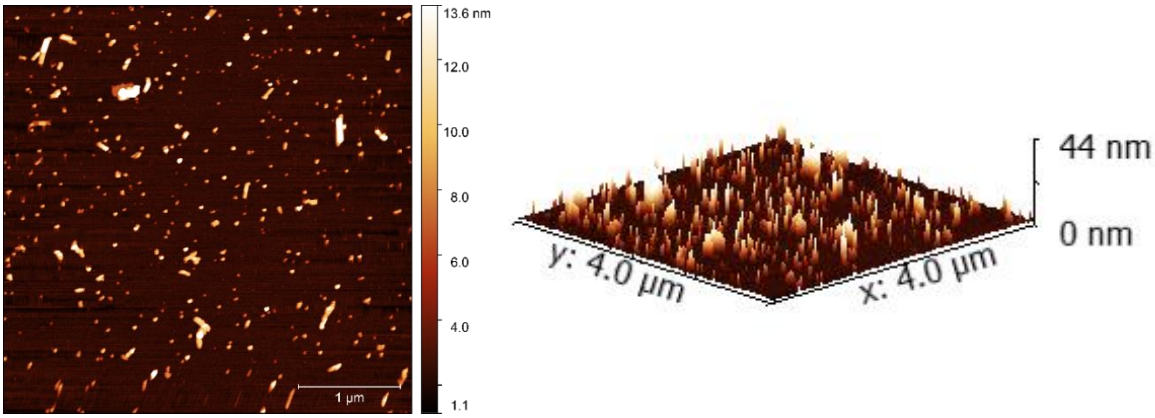

Figure S5. Two dimensional (left) and 3D (right) representations of AFM images of sonicated aS fibrils (wtaS:aS9 = 20:1) on a mica substrate.

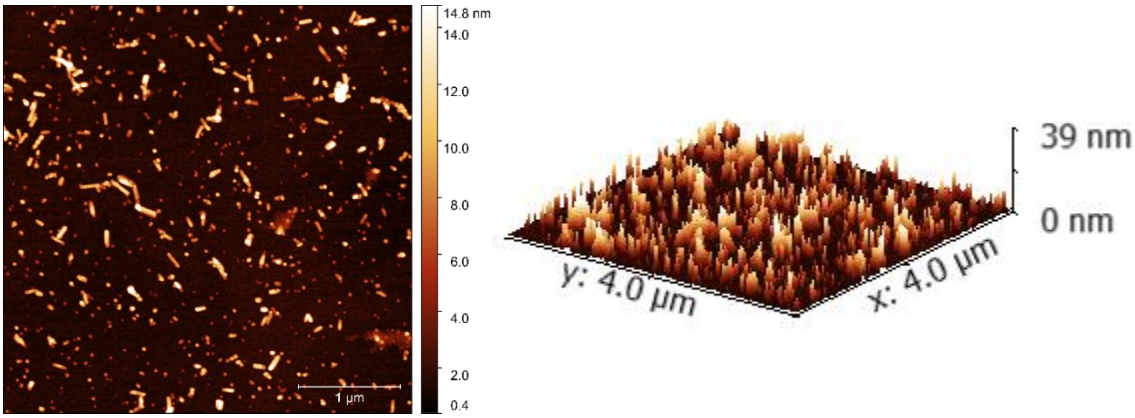

Figure S6. Two dimensional (left) and 3D (right) AFM images of aS fibrils (wtaS:aS69 = 20:1) on a mica substrate.

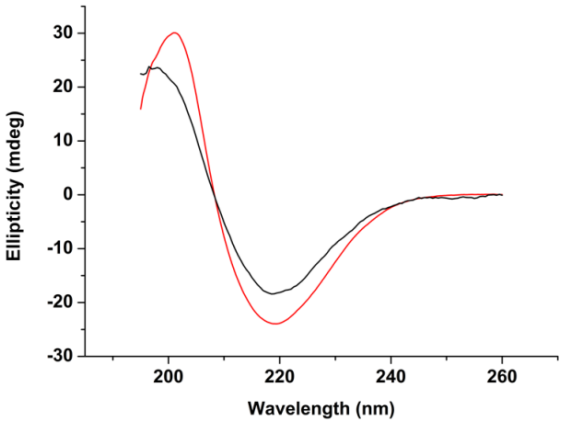

Figure S7. CD spectra of aS fibrils (wtaS:aS9 = 20:1) in black and aS fibrils (wtaS:aS69 = 20:1) in red in Tris-HCl (10 mM, pH 7.4, 100 µM EDTA, 150 mM NaCl) show β-sheet conformation of fibrillized aS.

3. Data analysis of cw-EPR spectra

All measured scans were baseline-corrected with a 2nd order polynomial.
Analysis of the spectra was performed using Matlab R2016a (The MatWorks, Inc. Natrick, MA) and the toolbox EasySpin 5.0.20[6].
For the aS fibril spectra all scans were accumulated because no signal decay was observed.
For the in-cell aS spectra, the optimum number of scans to accumulate was determined by optimizing the resulting signal-to-noise-ratio of the middle peak amplitude (see Figure S8).

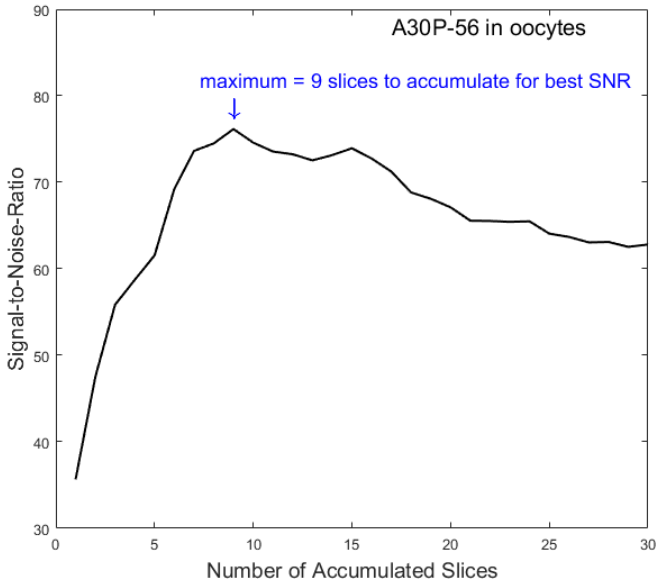

Figure S8. Signal-to-Noise-Ratio (SNR) of the exemplary accumulated cw-EPR spectrum slices to determine the maximum value of the SNR and thus the number of slices to accumulate.

The background spectrum was smoothed using a Savitzky-Golay filter and corrected for frequency deviations (see Fig S9).

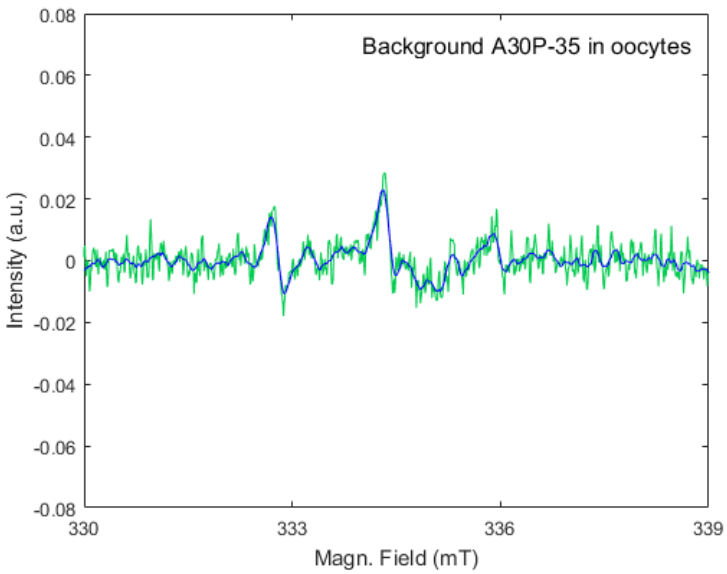

Figure S9. Background spectrum of A53T-35 injected into oocytes before (green) and after smoothing (blue). There is still some nitroxide signal left because the nitroxide is not fully reduced, yet.

The modified background spectrum was subtracted from the accumulated spectrum of the labeled aS variants injected into oocytes (see Figure S10-S12). In some background spectra there is still some nitroxide signal left because the time between the actual measurement and the background measurement was not long enough and the nitroxide is not fully reduced, yet (see Fig S9).

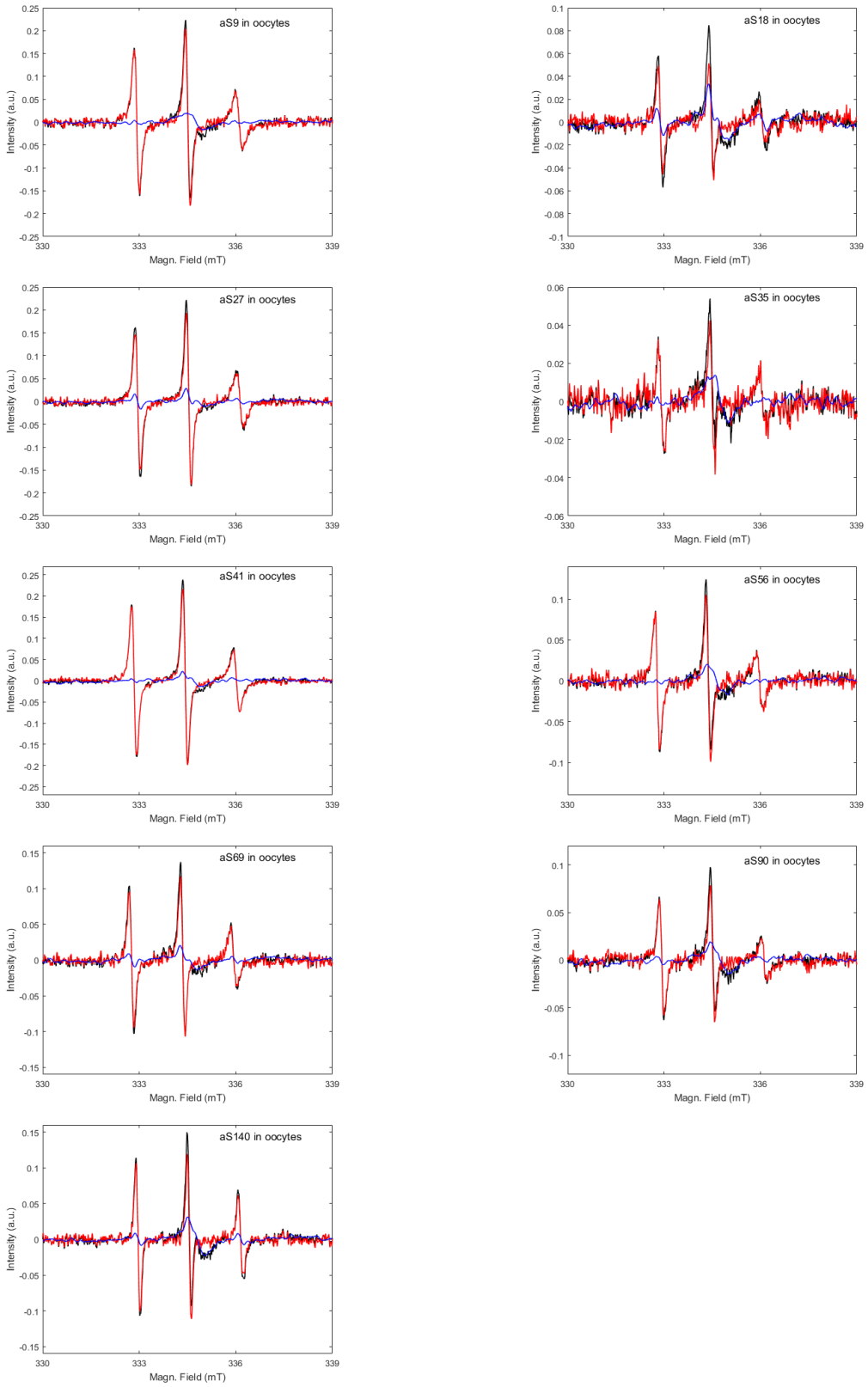

Figure S10. Accumulated cw-EPR spectra of aS wild-type injected into oocytes of *Xenopus laevis* (black), smoothed oocytes background (blue) and background-corrected spectra (red).

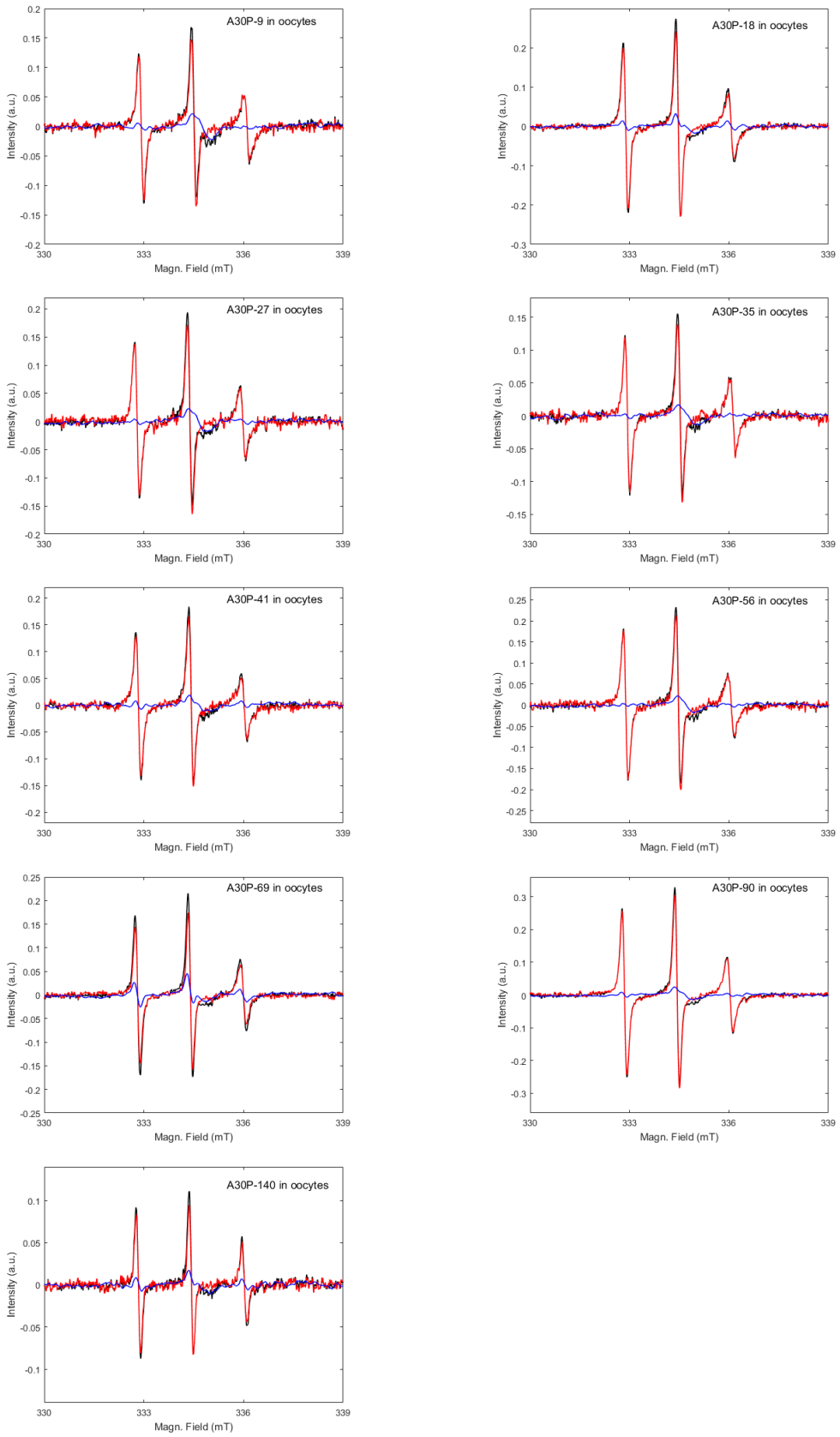

Figure S11. Accumulated cw-EPR spectra of A30P injected into oocytes of *Xenopus laevis* (black), smoothed oocytes background (blue) and background-corrected spectra (red).

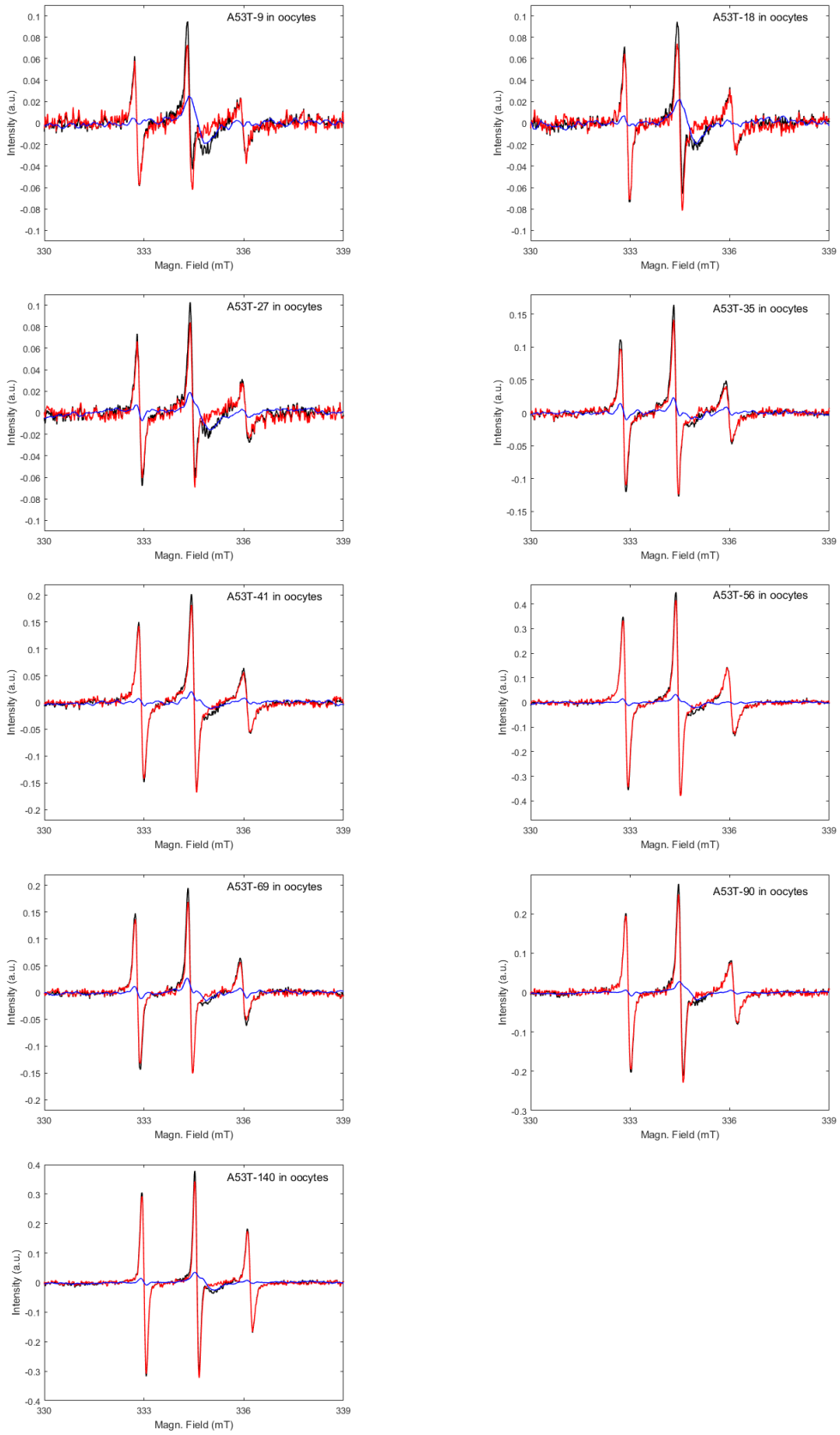

Figure S12. Accumulated cw-EPR spectra of A53T injected into oocytes of *Xenopus laevis* (black), smoothed oocytes background (blue) and background-corrected spectra (red).

4. Intracellular spatial distribution of aS

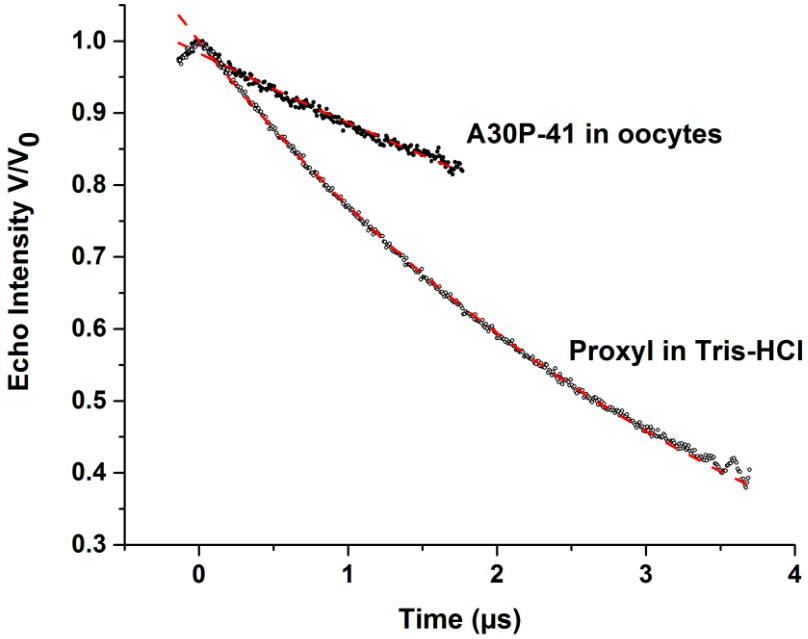

Figure S13. Four pulse DEER-traces of A30P-41 in oocytes (dots) and PROXYL in Tris-HCl (20 vol % glycerin) (as reference) (dots) and corresponding fits (dashed red lines). Concentration of PROXYL sample (reference sample) 414 µM, local concentration of A30P-41 165µM.

DEER measurements (see also part A, Chapter 10 for experimental details) were used to determine the spatial distribution of aS upon microinjection.

50.6 nL of A30P-41 with an initial spin concentration of 1.7 mM was injected into three oocytes (volume ~ 1 µL), respectively. The sample was incubated for 15 minutes and shock-frozen for the EPR measurement.
PROXYL in Tris-HCl bulk solution (20 vol% Glycerol) was used as reference. For determining the concentration of the reference sample a cw-EPR spectrum was measured using an EMXnano spectrometer (Bruker Biospin). A modulated field sweep containing 3333 data points (sweep time 84.72 s) at a modulation frequency of 100 kHz, 0.6 G modulation amplitude and a time constant of 20.48 ms at room temperature was performed. Spectrometer control and quantitative analysis were performed by the Bruker Xenon software. Using the spin calculation tool, included in the software, the concentration of the reference sample was determined to be 414 µM.

The corresponding DEER traces of A30P-41 and for the (shock frozen) reference sample are shown in Figure S13. Data analysis was performed using the DeerAnalysis_2016 software package for MATLAB and following the description in the DeerAnalysis2013b manual section 10.6.[7] The local spin concentration of A30P-41 was determined to be 165 µM 15 min after incubation.
Taking the intracellular lifetime of 17 min into account (see Figure S14) the dilution to 165 µM (local spin concentration) of A30P-41 results into an expansion of the injected volume to a volume of about 182 nL in the cell, which results in an expansion by factor 3.6 after 15 minutes of incubation before shock-freezing the sample.

5. Stability and line shape of the in cell nitroxide signal

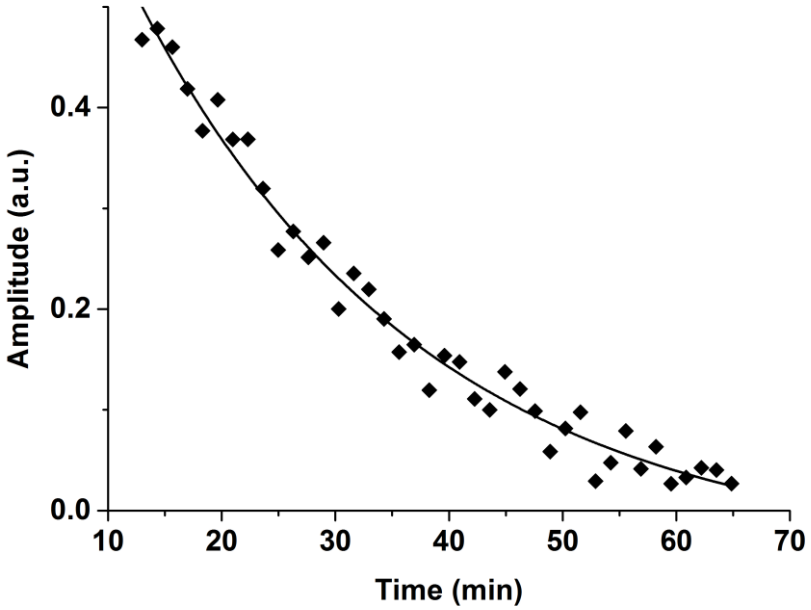

Figure S14. Time dependent signal intensity of spin-labeled aS upon microinjection into oocytes for A30P-41. The signal decays with a half-life of 17.6 ± 1.7 min.

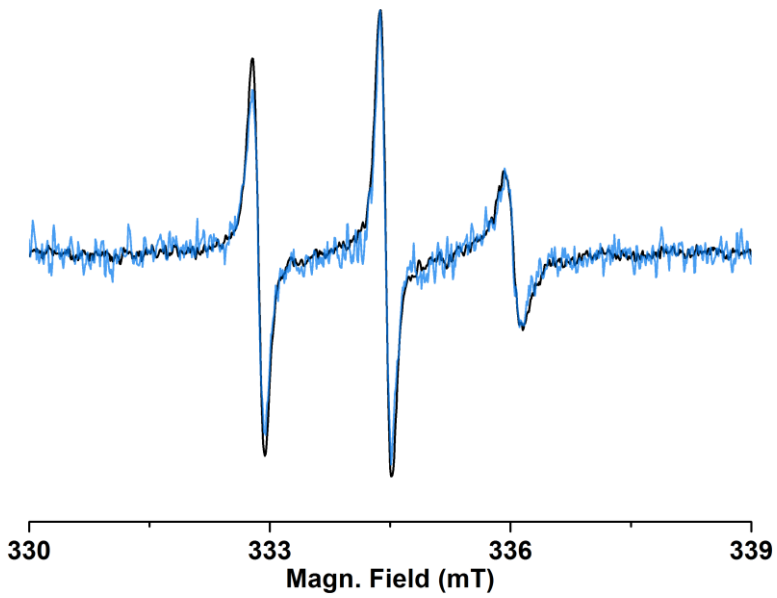

Figure S15. Normalized (by maximum) cw-EPR spectra of A53T-56 injected into oocytes accumulated in the period measured 12-20 min (black) and 51-62 min (blue) after injection, respectively.

6. 4-Oxo-Tempo as viscosity control inside the cell

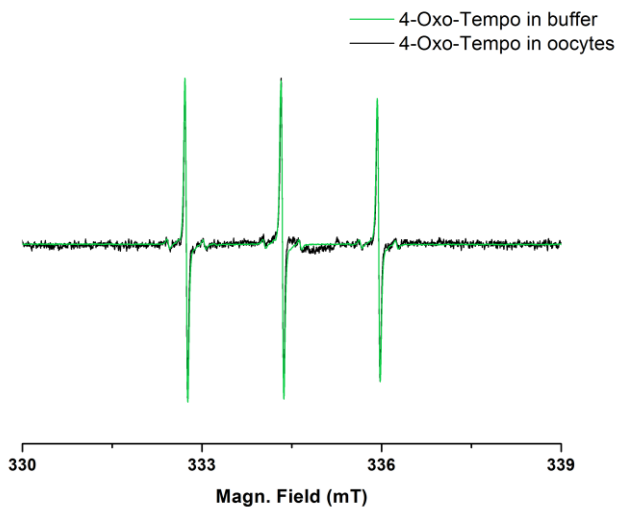

Figure S16. Cw-EPR spectrum of 4-Oxo-Tempo (Tempone) in buffer (green) and injected into oocytes (black).

Analysis of the spectrum was performed using Matlab R2016a (The MatWorks, Inc. Natrick, MA) and the toolbox EasySpin 5.0.20[6]. The spectrum of 4-Oxo-Tempo in buffer was simulated using the EasySpin function *garlic*. A similar simulation with an increased rotational correlation time τ (by factor 1.2) assuming an increase in viscosity by factor 1.2 was done (see Figure S17 and Table S6) to mimic the viscosity increase in the cell. The simulation proves the change in viscosity inside the cell is negligible and does not result in significant spectral changes in the cw-EPR spectrum.

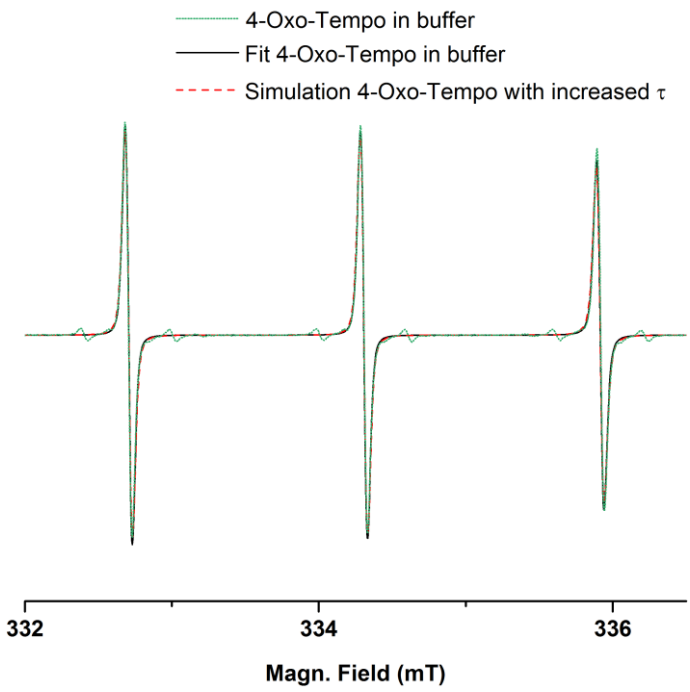

Figure S17. Cw-EPR spectrum of 4-Oxo-Tempo in buffer (green, dotted line), corresponding simulation (black, solid line), and simulation with increased rotational correlation time assuming an increase in viscosity by factor 1.2 (red, dashed line)[8]. For simulation parameters see Table S6.

Table S6 Parameters of simulating 4-Oxo-Tempo in buffer and spectral simulation parameters for changed viscosity (≈ rotational correlation time) inside oocytes by a factor of 1.2, both shown in Fig S9. All simulations were done with 0.046 mT linewidth and g-tensor = [g_x g_y g_z] = [2.0268 2.0033 1.9897].

	^{14}N Hyperfine coupling Constant [MHz]		**Rotational correlation time [ns]**
	A_{xx}=A_{yy}	**A_{zz}**	**τ_r**
4-Oxo-Tempo in buffer	18	98	0.018
4-Oxo-Tempo with changed viscosity	18	98	0.021

7. Comparison of in-cell EPR spectra and spectra in aqueous solution

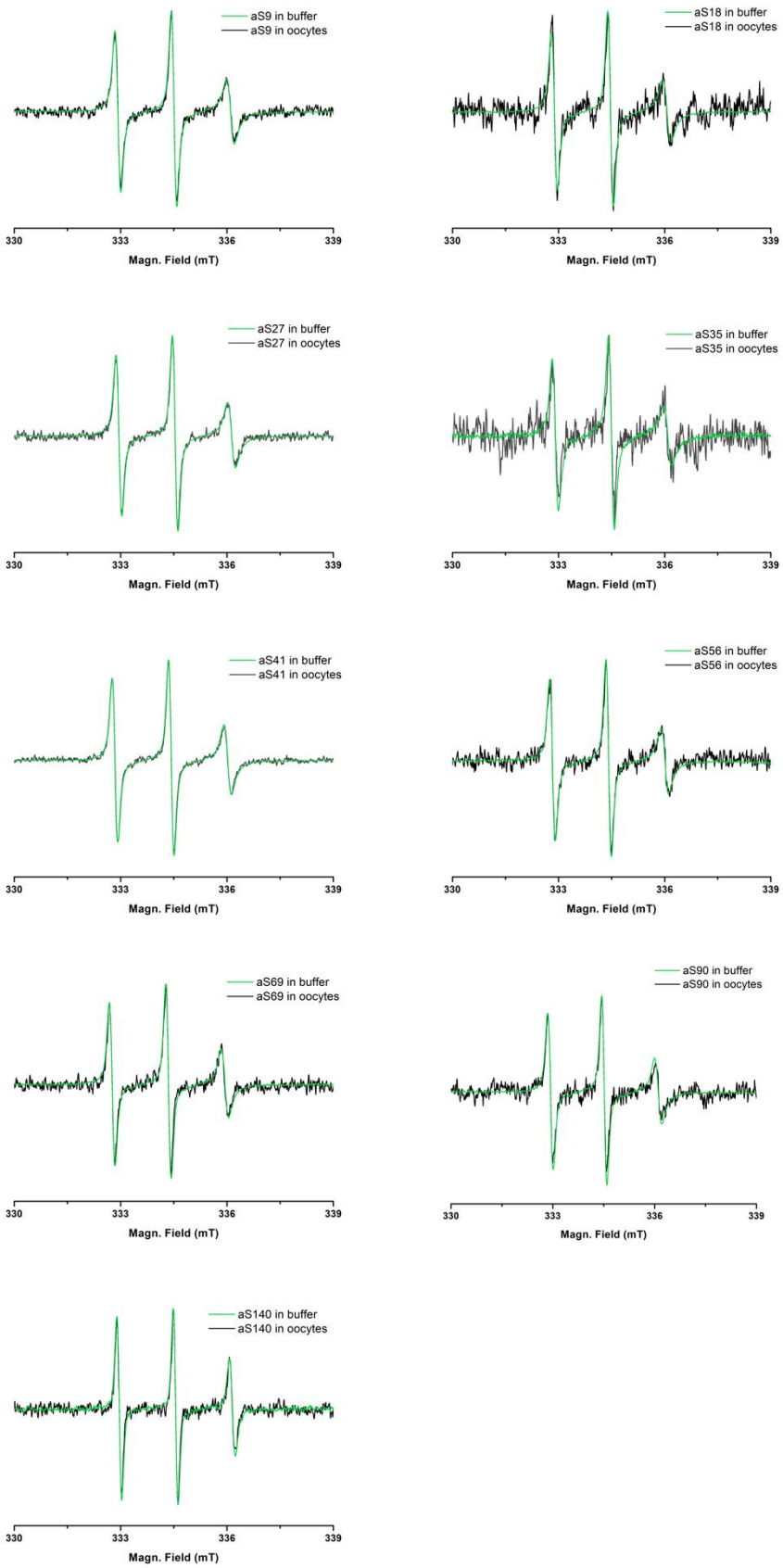

Figure S18. Cw-EPR spectra of aS (labeled at various positions) in buffer (green) and injected into oocytes upon background correction (black).

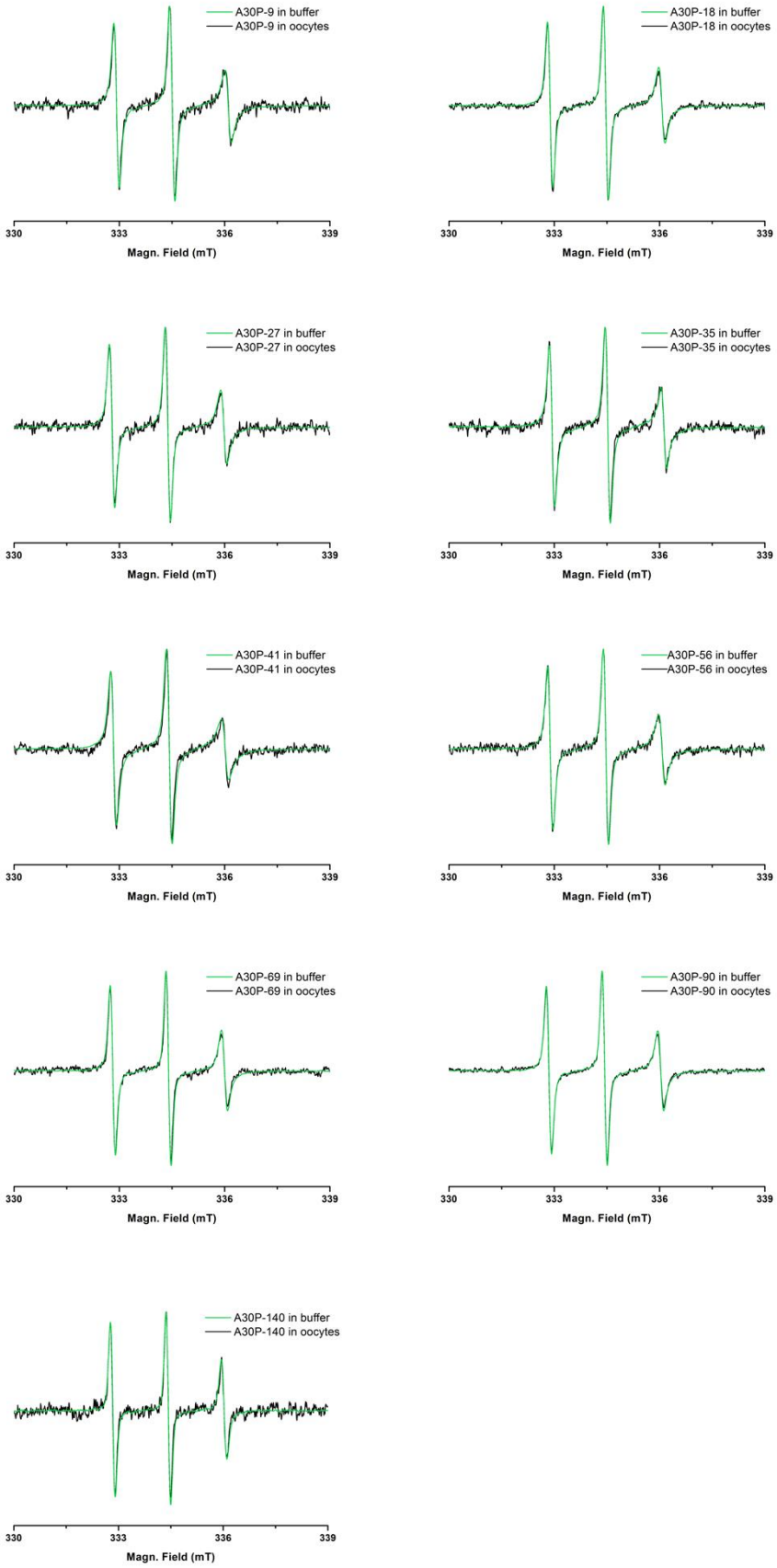

Figure S19. Cw-EPR spectra of A30P (labeled at various positions) in buffer (green) and injected into oocytes upon background correction (black).

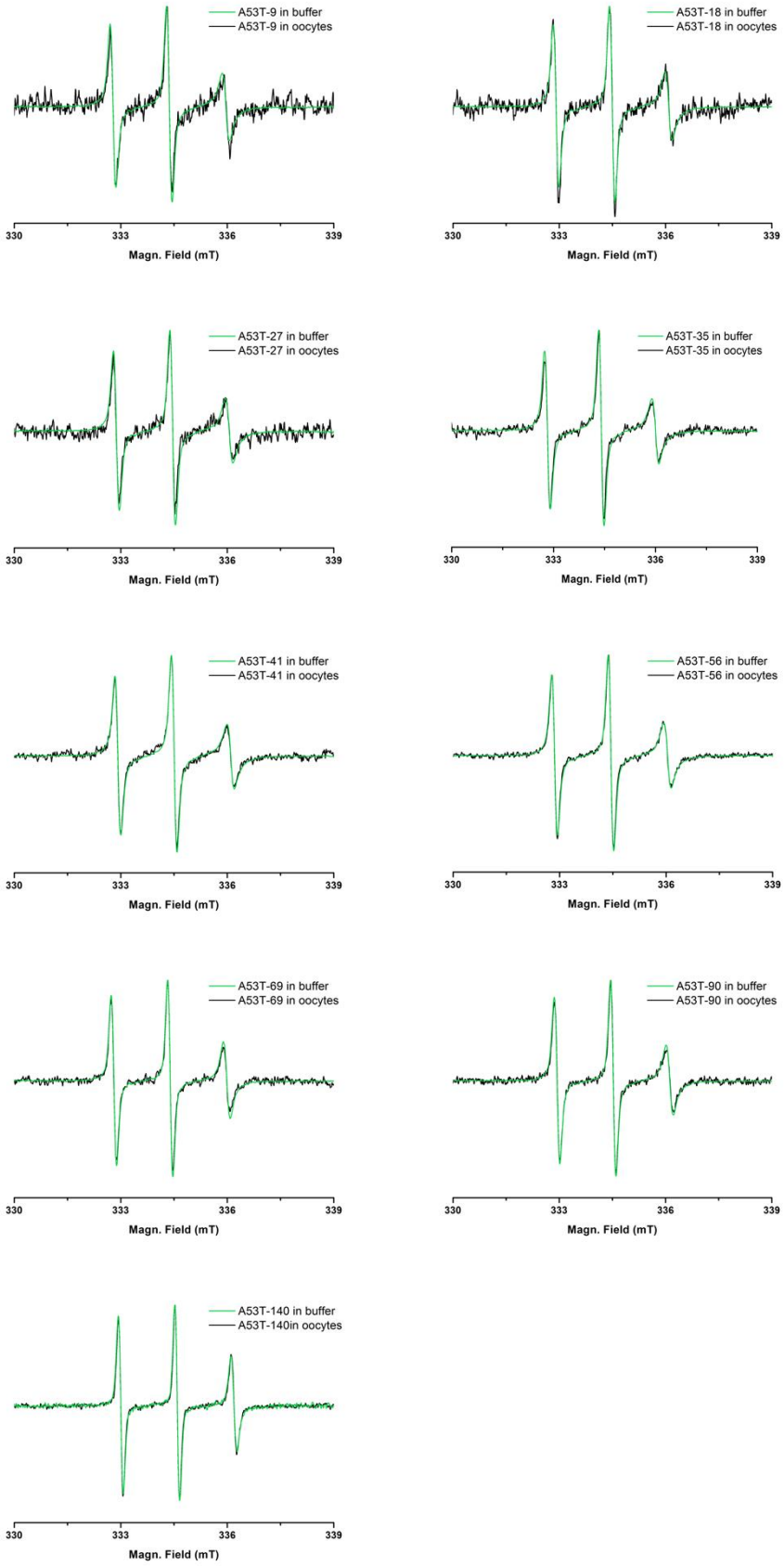

Figure S20. Cw-EPR spectra of A53T (labeled at various positions) in buffer (green) and injected into oocytes upon background correction (black).

8. Comparison of in-cell wild-type aS with A30P and A53T

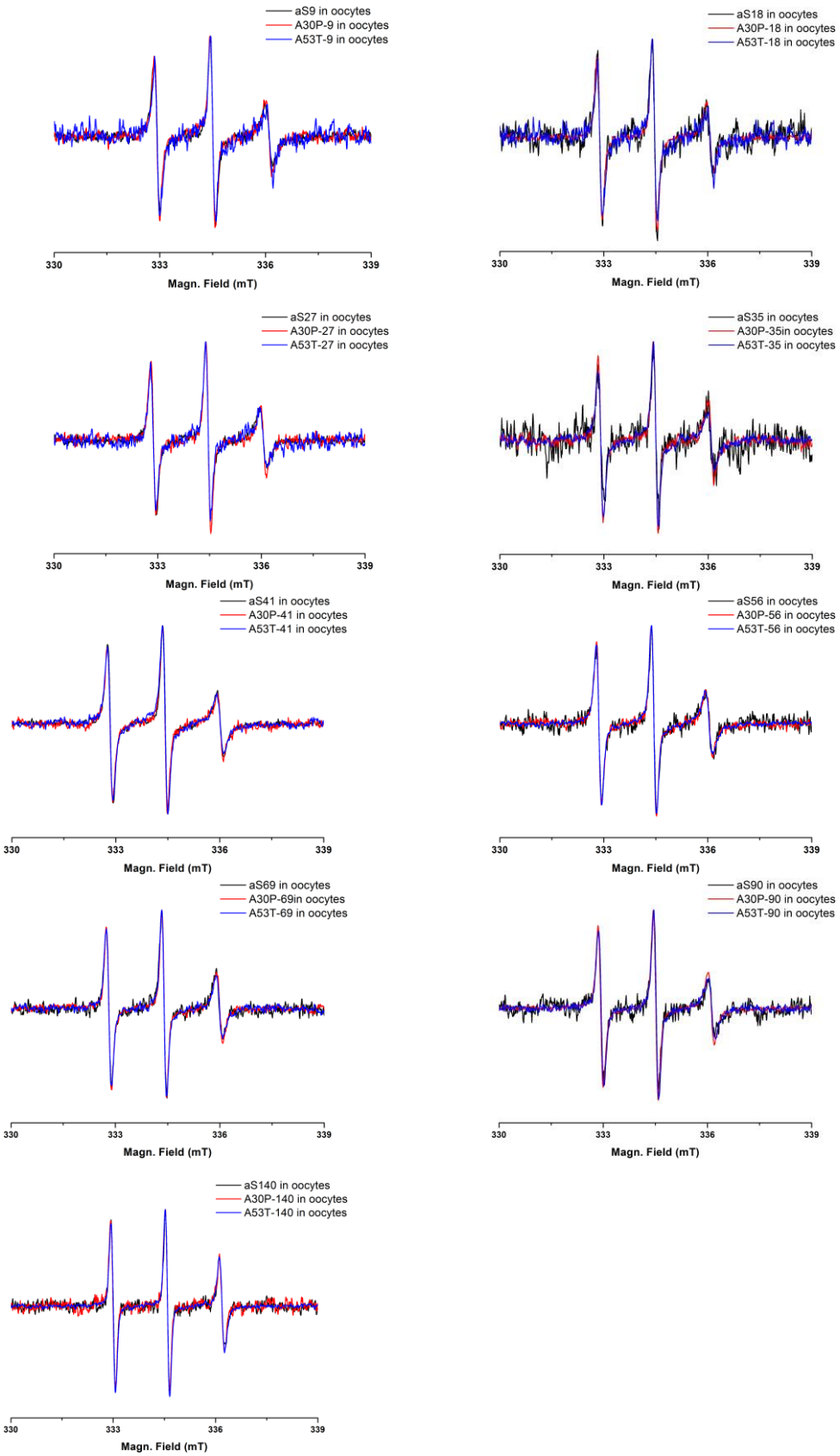

Figure S21. Intracellular cw-EPR spectra of wt-aS (black), A30P (red) and A53T (blue) spin-labeled at position 9, 18, 27, 35, 41, 56, 69, 90, 140, respectively.

9. Quantitative spectral analysis of the intracellular experiments

Hidden in the noise of the intracellular EPR spectra might be an aS fraction which adapted a defined order, e.g. membrane bound or fibrillized. In order to determine the upper limit of this fraction, we performed spectral simulations with varying contributions of the corresponding spectral components as derived from the control experiments (see Table S4 and S5).

Figure S22 shows several simulations with varying ratios of S_A (intrinsically disordered) and S_B (membrane bound) as well as experimental data (aS9 in oocytes).

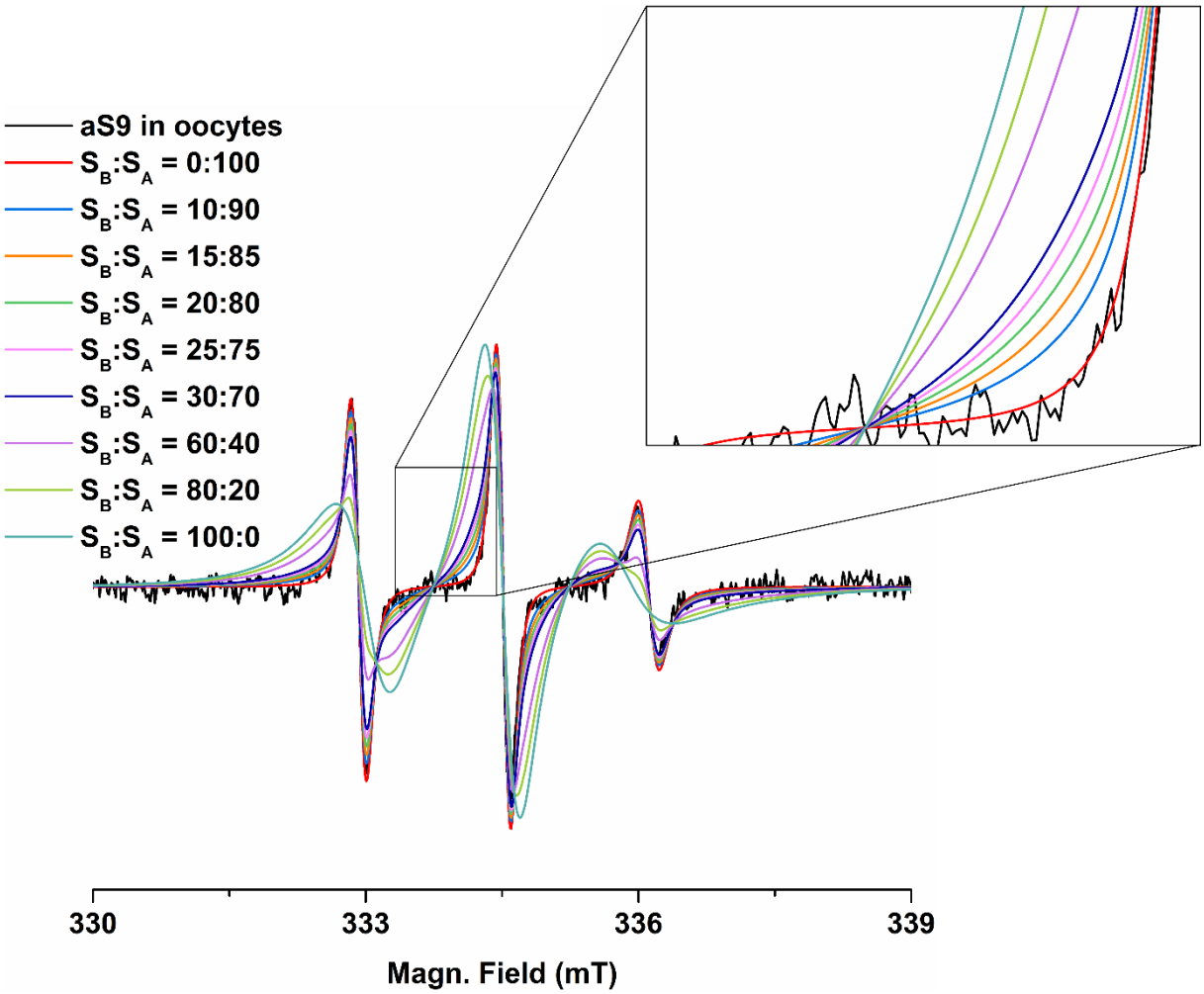

Figure S22. Spectrum of aS9 injected into oocytes upon background correction (black) and spectral simulation of different ratios of the monomeric, intrinsically disordered spectral component S_A and the alpha-helically membrane bound spectral component S_B.

Simulated spectra with different ratios of the component S_A and the fibril components S_D, S_E and S_G taken together in an overall fibril component S_F (all obtained fitting parameters and ratios were kept) for aggregated aS69 were simulated and compared with the spectrum of aS69 in oocytes (see Figure S23).

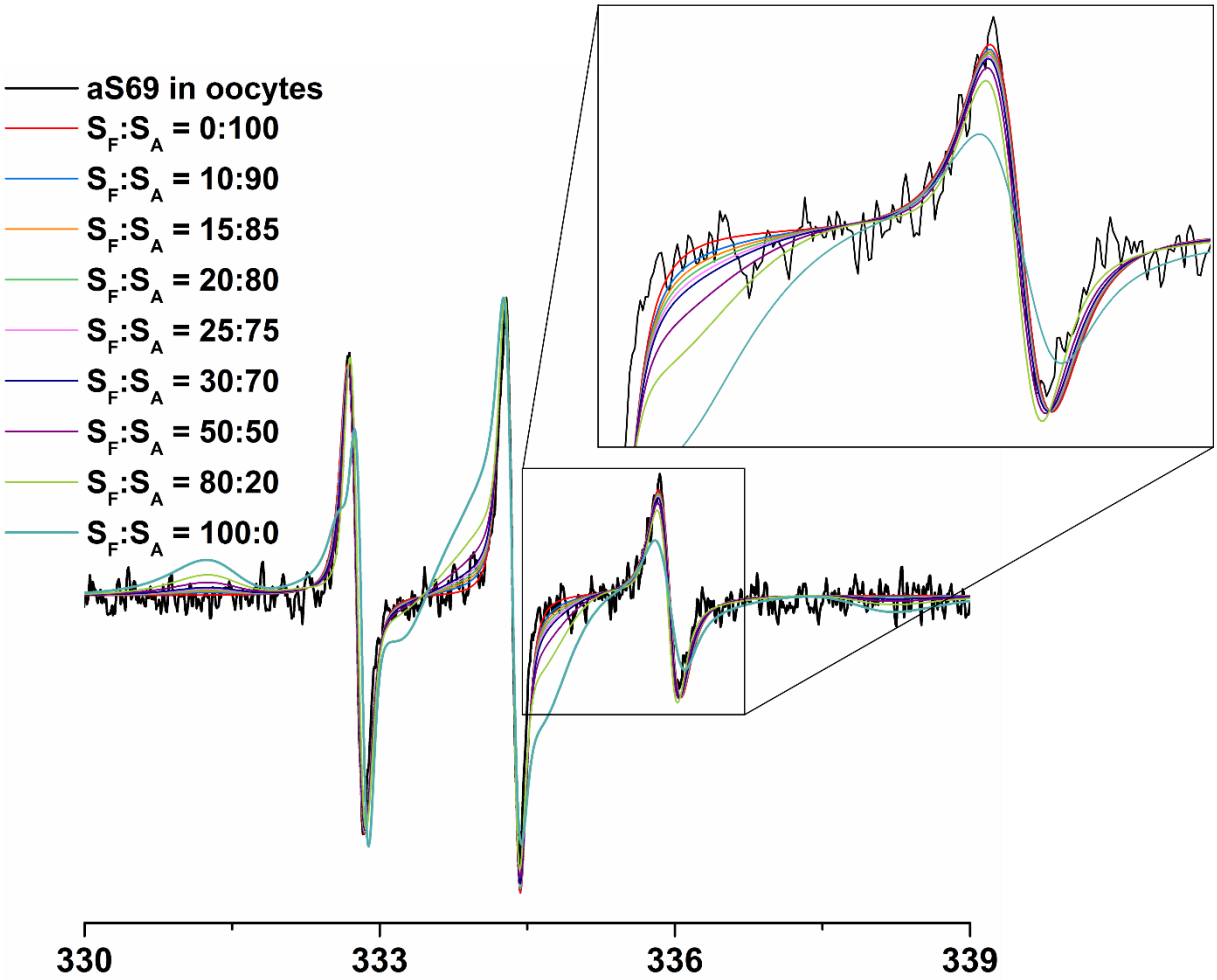

Figure S23. Spectrum **of** aS69 injected into oocytes upon background correction (black) and spectral simulation of different ratios of a monomeric, intrinsically disordered spectral component S_A and a fibril component S_F.

C. REFERENCES

1 M. E. van Raaij, I. M. J. Segers-Nolten and V. Subramaniam, *Biophys. J.*, 2006, **91**, L96-98.
2 P. S. Chen, T. Y. Toribara and H. Warner, *Anal. Chem.*, 1956, **28**, 1756–1758.
3 G. Jeschke, *Annu. Rev. Phys. Chem.*, 2012, **63**, 419–446.
4 M. I. Iurascu, C. Cozma, N. Tomczyk, J. Rontree, M. Desor, M. Drescher and M. Przybylski, *Anal. Bioanal. Chem.*, 2009, **395**, 2509–2519.
5 M. Drescher, B. D. van Rooijen, G. Veldhuis, V. Subramaniam and M. Huber, *J. Am. Chem. Soc.*, 2010, **132**, 4080–4082.
6 S. Stoll and A. Schweiger, *J. Magn. Reson. San Diego Calif 1997*, 2006, **178**, 42–55.
7 G. Jeschke, V. Chechik, P. Ionita, A. Godt, H. Zimmermann, J. Banham, C. R. Timmel, D. Hilger and H. Jung, *Appl. Magn. Reson.*, 2006, **30**, 473–498.
8 Y. Ye, X. Liu, Y. Chen, G. Xu, Q. Wu, Z. Zhang, C. Yao, M. Liu and C. Li, *Chem. - Eur. J.*, 2015, **21**, 8686–8690.